

Performance Evaluation of Wavelet Based Coders on Brain MRI Volumetric Medical Datasets for Storage and Wireless Transmission

D. Dhouib, A. Naït-Ali, C. Olivier and M. S. Naceur

Abstract—In this paper, we evaluate the performance of some wavelet based coding algorithms such as 3D QT-L, 3D SPIHT and JPEG2K. In the first step we achieve an objective comparison between three coders, namely 3D SPIHT, 3D QT-L and JPEG2K. For this purpose, eight MRI head scan test sets of 256 x 256x124 voxels have been used. Results show superior performance of 3D SPIHT algorithm, whereas 3D QT-L outperforms JPEG2K.

The second step consists of evaluating the robustness of 3D SPIHT and JPEG2K coding algorithm over wireless transmission. Compressed dataset images are then transmitted over AWGN wireless channel or over Rayleigh wireless channel. Results show the superiority of JPEG2K over these two models. In fact, it has been deduced that JPEG2K is more robust regarding coding errors. Thus we may conclude the necessity of using corrector codes in order to protect the transmitted medical information.

Keywords—Image coding, medical imaging, wavelet based coder, wireless transmission.

I. INTRODUCTION

NOWADAYS, medical volumetric data produced by different imaging modalities are continually increasing.

The representation of such images can be either bidimensional or tridimensional (i.e. volumetric). Therefore, in case of volumetric data, imaging techniques, such as Computed Tomography (C.T), Magnetic Resonance Imaging (MRI), provide an image set which represents a certain number of slides of a given part of human anatomy.

In telemedicine applications, the huge amount of data can complicate both transmission and storage process [1][2]. In fact, face to low channel bandwidth and storage cost, it is generally recommended to reduce both transmission bitrate and storage space [3, 4]. Thus, in this context, various efficient compression techniques have been developed in the last decades.

D. D. Author is with Université de Poitiers, SIC of XLIM Laboratory UMR CNRS 6172, France and Ecole Nationale d'ingénieurs de Tunis, LTSIRS Laboratory, B.P. 37 le Belvédère 1002 .Tunisia, (e-mail: dhouib@sic.sp2mi.univ-poitiers.fr).

A. N. Author, is with Université de Paris 12, LiSSi EA 3956 laboratory, France, (e-mail: naitali@univ-paris12.fr).

C. O. Author is with Université de Poitiers, SIC of XLIM Laboratory UMR CNRS 6172, France, (e-mail: olivier@sic.sp2mi.univ-poitiers.fr).

M. S. N. Author is with Ecole Nationale d'ingénieurs de Tunis, LTSIRS Laboratory, B.P. 37 le Belvédère 1002 .Tunisia, (e-mail: naceurs@yahoo.fr).

The trend in image compression is increasingly wavelet-based due to the fact that it provides high image quality at high compression rates [5]. Therefore, several image coding algorithms have been proposed in the literature, including Embedded Zerotree Wavelet (EZW) algorithm [6, 7]. In fact, EZW algorithm has been proposed by Shapiro in 1993 and was the first efficient and elegant subband coding algorithm by zerotree. On the other hand, SPIHT is an improvement of EZW and has been proposed by Said and Pearlman [8-9]. Moreover, The Set Partitioned Embedded bloCK coder (SPECK) [10, 9] proposed by Pearlman and al., which uses wavelet packet transform, can be compared to SPIHT and use an insignificant coefficient set block structure so the difference between the two methods concerns mainly the partitioning of wavelet coefficients.

In addition, one can evoke EBCOT [11] for: Embedded Block Coding with Optimal Truncation [12-15] and QuadTree Limited (QT-L) [16,17] coder which is the combination of two techniques, the quadtree coding and the block-based coding of the significance maps.

Many of these algorithms were extended to 3D, namely the multidimensional layered zerotree coding (MLZC) [18, 19], the 3D-SPIHT [16, 20, 21] and the 3D-QLT [16, 17].

In this study, we will be focusing on 3D SPIHT, 3D QT-L and JPEG2000.

The last three coders can reduce the number of bits required to represent the medical image dataset, but they may introduce some distortion, which will cause a possible loss of useful clinical information. This may influence significantly diagnosis [22]. Thus, these three coders will be compared in terms of performances.

One has to point out that major goals in telemedicine consist in allowing efficient remote processing of compressed medical images [23], basically if such application is integrated into mobile devices [24]. Therefore, in this work, we will be interesting in evaluating the robustness of compressed images face to coding errors over a wireless transmission channel [25-29].

This paper is organized as follows. Section 2 provides a brief overview on the three different evaluated wavelet-based coders, namely 3D-SPIHT, 3D-QLT and JPEG2000. For this purpose, channel transmission models such as Gaussian and Rayleigh have been used. In section 3, details about

experimental results and discussion will be presented. Finally, a conclusion about the obtained results is carried out in section 4.

II. MATERIALS AND METHODS

A. Image selection

In this paper, only MRI data will be considered. The compression performances of the proposed coders were evaluated on eight sets of volumetric data. Each MRI image dataset is 256 x 256 x 124. In addition, each pixel is represented by 8 bits. Different brain tumour cases are considered. Those data sets are provided from the new medical image and signal database, Medical Database for the Evaluation of Image and Signal processing (MeDEISA) [30].

B. The coding algorithm

Generally, wavelet Transform-based image data compression involves the following successive steps [31] (Fig. 1):

Transformation: a reversible transformation is applied to the image in order to convert it into another domain which allows an efficient decorrelation of information,

Quantization: the values obtained from the previous step are approximated to integer values in order to reduce their range. This will allow a reduction of bit rate [32]. In addition, this phase is considered irreversible which causes systematically data loss. The quantization can be either scalar or vectorial,

Entropy coding: in this step data are encoded according to a lossless method.

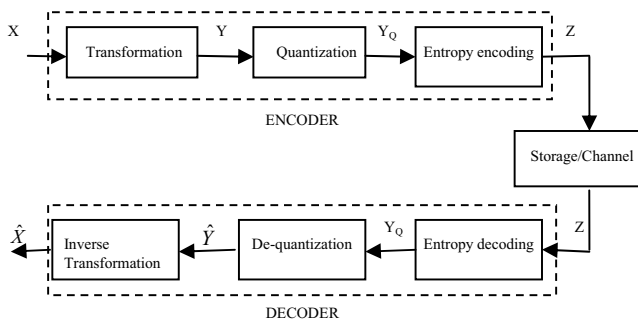


Fig. 1 Generic compression scheme

1) 3D-SPIHT

The 3D-SPIHT algorithm is a modified version of SPIHT technique, which is a 3D extension of the well know SPIHT coding algorithm. Like the EZW algorithm, SPIHT technique proposed by Shapiro [6] supports progressive data transmission [5]. In addition, EZW as well as SPIHT are embedded techniques; the produced embedded bitstream can be truncated at any point. In other words, the compression process can be stopped at a desired rate [7]. Both algorithms consider wavelet coefficients as a collection of spatial orientation trees. Each tree is composed of coefficients from all subbands corresponding to the same spatial location in an image [21]. The image wavelet coefficients are scanned in the usual order, column then line, from low subbands to high

subbands. They are based on an iterative algorithm which selects an initial threshold based on the largest wavelet coefficient [7]. A tree wavelet coefficient set is said significant if the largest coefficient magnitude in the set is greater than or equal to the selected threshold. The SPIHT coding algorithm is performed on two passes, called sorting pass and refinement pass. SPIHT perform a recursive partitioning of the tree in such a way that it allows identifying the position of significant coefficient in the descendants of the considered coefficient [4]. During the sorting pass, the coefficients in the list of insignificant pixels (LIP) are sorted and those that become significant after changing the threshold are moved to a list of significant pixels (LSP). Similarly, wavelet coefficients of the LIP list are moved when the most significant bit (MSB) set to 1 is encountered in the sorting pass. During the refinement pass, the remaining bits following the first significant bit are output. The iterative algorithm is repeated by decrementing the threshold which is usually a power of 2 each time and terminated when the minimum threshold is reached.

As it has been said before, SPIHT is the core element of 3D-SPIHTs [25] algorithm which is proposed by Kim and al.. The basic difference between the two coders is that the first one processes 3D wavelet coefficients as a collection of 3D spatial orientations tree (Fig. 2) and that context modelling in arithmetic coding is more involved [21]. 3D transforms are performed by applying sequentially the 1D transform across the three dimensions. Each node in the spatial-temporal orientation tree is a group representation of eight wavelet coefficients forming a 2x2x2 adjacent group [21]. For 3D wavelet transformation, every 16 frames form a Group Of Picture (GOP). The selected context models are based on the significance of the individual node members and the state of their descendants. Thus, four state combinations are possible for each node coefficient, which result in total of 164 different context models [16].

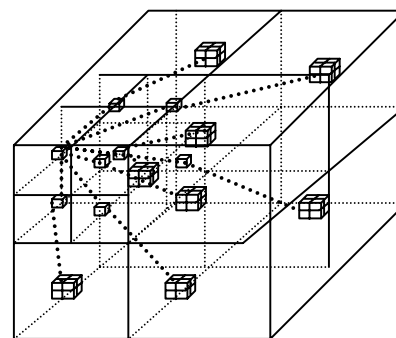


Fig. 2 3D spatial orientation tree

2) 3D QT-L

The 3D QT-L [33] is an intraband coding algorithm based on block partitioning of the 3D wavelet transform which is an extension of the 2D QT-L. 3D QT-L builds octrees corresponding to each significance map. The same partitioning rule as CS is used recurrently on cube of 3D

wavelet transform. The cube splitting algorithm is a 3D version of the SQP algorithm. SQP coding [17] is based on Successive Approximation Quantization (SAQ) and use the quadtree coding of the significance maps. Encoding the significance maps, in other words the positions of the significant coefficients is equivalent to the encoding of the corresponding quadtrees.

For the 3D QT-L coding, the partitioning process is limited in such a way that once the volume of a node becomes smaller than a predefined threshold volume, the splitting process is stopped and the entropy coding of the coefficients within such a significant leaf node is activated [16].

This coding algorithm is performed on three passes; the significance pass, the refinement pass and finally the non significant pass. During the significance pass of one given bit plane, the coordinates of the non significant coefficient found in a significant node are appended into a List of Nonsignificant Coefficients (LNC). During the next coding steps, the significance of the LNC list coefficients is coded first. Depth-first scanning is used to scan the octrees. The eight descendant nodes of any given parent node are scanned using a 3D instantiation of the Morton-curve.

The context conditioning phase and context-based entropy coding of the symbols generated in the three coding passes are more elaborated.

Four different model sets are used in order to encode generated symbols and the encoder automatically chooses the appropriated set to each coding stage.

3) JPEG2000

JPEG2000 [12, 14] is the last image compression standard designed to support a variety of applications, including the compression and transmission of medical images. The international standard JPEG2000 [12] is based on the dyadic discrete wavelet transform (DWT). The DWT can be reversible (le Gall (5,3) taps filter) or irreversible(Daubechies (9,7) taps filter) [15]. After that, scalar quantization step is performed which quantize all coefficients. The quantizer follows an embedded dead-zone scalar approach and is independent for each subband. Then, for entropy coding stage, a contextual adaptatif arithmetic coder is used. Finally the rate allocation step and bitstream organisation are based on EBCOT algorithm [13,].

EBCOT is the basic encoding engine of JPEG2000 which is proposed by Taubman in 2000 [11]. EBCOT is based on two passes, where each subband data is partitioned into small independent blocks, called code-blocks of medium size (32 x 32 or 64 x 64). Those code blocks are coded on highly progressive bit stream and truncation points are saved in the second pass of rate-distortion optimisation. Each block is separately encoded, thus it result on a separately embedded and layered bit-stream organization. Each code-block bit-stream is truncated in an optimal way so as to minimize distortion subject to the bit-rate constraint. The constructed bitstream is organized as a succession of layers which contains additional contributions from each block (some contributions

might be empty). Block truncation points associated with each layer are optimal in the rate distortion sense. Each bloc is coded in progressive way in bit plane. They are divided into 16x16 sized sub-blocks. Each bit-plane is encoded in four passes namely the forward significance propagation pass, the reverse significance propagation pass, the magnitude refinement pass and the normalization pass. The embedded block coding strategy is based on four different primitive coding operations such as Zero Coding (ZC), Run-Length Coding (RLC), Sign Coding (SC) and Magnitude Refinement (MR) which are called in the coding passes in order to code new information for a single sample in bit-plane.

C. Transmission

Image transmission over wireless channels is based on several channel models. For example, one can cite some simple models as Binary Symmetric Channel (BSC) and Additive White Gaussian Noise (AWGN). On the other hand, more efficient models can be used as Rice and Rayleigh [27].

1) AWGN channel

The AWGN canal is the widely used continue channel model. A Gaussian white noise is added to transmitted signal. This kind of noise come from two sources, the intern one generates thermique noise, which is caused by electrons pass inside electronic device and the extern one which is produced by different radiances captured by emission and reception antenna. Those noises are modelled by a stationary random process $n(t)$ which is added to signal. Thus, this signal follows the following probability density function $P(n)$:

$$P(n) = \frac{1}{\sqrt{2\pi\sigma^2}} \exp\left(-\frac{n^2}{2\sigma^2}\right) \quad (1)$$

Where:

σ^2 is the signal total power,

n is the Gaussian white noise with $DSP=N_0/2$,

For the AWGN channel, the simulation model is given by (Fig. 3).

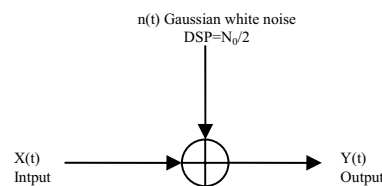


Fig. 3. Gaussian channel modeling

$$y(t)=x(t)+n(t) \quad (2)$$

Where $y(t)$ is the signal noisy version and $x(t)$ is the transmitted signal.

2) Rayleigh fading channel

Multipath fading is a common scenario in wireless channel causing by Rice or Rayleigh fading [27]. Rayleigh fading channel is one of several statistical channels modelling radioelectrical transmission channel. The received signal is modelled as complex Gaussian process with average equal to

zero (i.e. no path are dominant to others) in which is added Gaussian additive white noise (Fig. 4.).

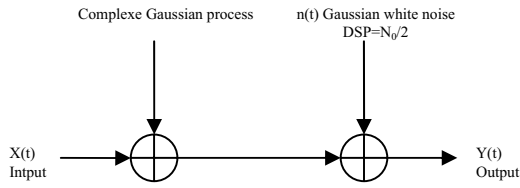


Fig. 4. Rayleigh channel modelling

The probability density function of the magnitude of the received signal following a Rayleigh law $P(s)$ is expressed by the following mathematical formula.

$$P(s) = \frac{s}{\sigma^2} \exp\left(-\frac{s^2}{2\sigma^2}\right) \quad (3)$$

Where σ^2 is always the total power of signal.

D. Evaluation

In case of irreversible (i.e. lossy) compression algorithms, reconstructed image is modified with some distortions depending of course on the compression ratio. Therefore, in order to evaluate and compare different coding process, we must evaluate the loss level, which allow controlling the reconstructed image quality.

In medical domain, details loss may cause a loss of useful clinical information leading in some cases to a possible erroneous diagnosis. According to American College of Radiology [34], clinically significant diagnostic information doesn't must be loss during compression process and must be performed under the direction of qualified physician. Thus, finding an acceptable distortion level is a great challenge which is according to [35] is dependant on kind of medical imaging modality used, coding algorithm, image acquisition protocol, explored organ, pathology.

There are some distortion or quality measures which allow comparing compression algorithm performances. Two of the error metrics are generally used. For instance, one can use the Mean Square Error (*MSE*) or the Peak Signal to Noise Ratio (*PSNR*). The *MSE* is the cumulative squared error between the compressed and the original image.

$$MSE = \frac{1}{MN} \sum_{y=1}^M \sum_{x=1}^N [X(x,y) - \hat{X}(x,y)]^2$$

Whereas *PSNR* is a measure of the peak error. *PSNR* measure allows the compression efficiency measuring because it is proportional to the quality.

$$PSNR = 20 * \log_{10}\left(\frac{255}{\sqrt{MSE}}\right) \quad (5)$$

Where $X(x,y)$ is the original image, $\hat{X}(x,y)$ is the decompressed image and M, N are the dimensions of the images.

A low value for *MSE* means a high *PSNR*. Of course, it is well known that these measures are, global rather than local.

III. EXPERIMENTAL RESULTS AND DISCUSSION

In this work, two experiments have been performed. The first one was the performance evaluation of compression algorithms enumerated previously in section 2.2. such as 3D QT-L, 3D SPIHT and JPEG2K. The performance evaluation is achieved on eight MRI head scan test sets of 256 x 256 x 124 voxels. The second experiment is the robustness evaluation of 3D SPIHT and JPEG2K coding algorithm over wireless transmission. This evaluation is performed in only one test dataset among the eight. The dataset images are compressed by one of the two coders. These compressed dataset images are transmitted either over AWGN wireless channel or Rayleigh wireless channel.

An interleaving process is added to model channel. This is a very used technique in many digital communications system. For an input symbol sequence, this process product an output symbol sequence equally sized, but with completely different temporal order. Thus interleaving process is a system which permutes sequence elements without any modification or redounding. The interleaving role in our model is to transform the engendered clustered error by the channel into distributed error over the sequence totality.

A. Results of compression

The performances of 3D-QT-L, 3D-SPIHT and JPEG2K have been analyzed for different bitrate values over the eight MRI data sets. Each dataset presents different brain tumor case. The information related to the evaluated datasets is presented in section 2.1. The *PSNR* is measured at seven different bit-rates: 2, 1, 0.5, 0.25, 0.125, 0.0625, and 0.03125 bits per pixel (bpp). We must point out that the three data sets are provided from the same medical imaging modality and acquired with the same acquisition protocol but the difference is that they present different patient with various tumour localisations.

Fig. 5 shows the variation of *PSNR* in decibels calculated for the eight data sets with respect to bitrate for the three coders 3D SPIHTs, 3D QT-L and JPEG2K. We observe that 3D SPIHTs algorithm outperforms the other coders for the eight datasets, for all bitrate values and for all the datasets except for the dataset number 3 (Fig. 5.c).

For this dataset (dataset number 3), 3D QT-L and 3D SPIHT achieve relatively the same result. At high rates (e.g. 2dB), JPEG2K outperforms the other coders, and the three coders are intersected.

For the other datasets, the *PSNR* provided by 3D QT-L coder are higher than those obtained by JPEG2K algorithm.

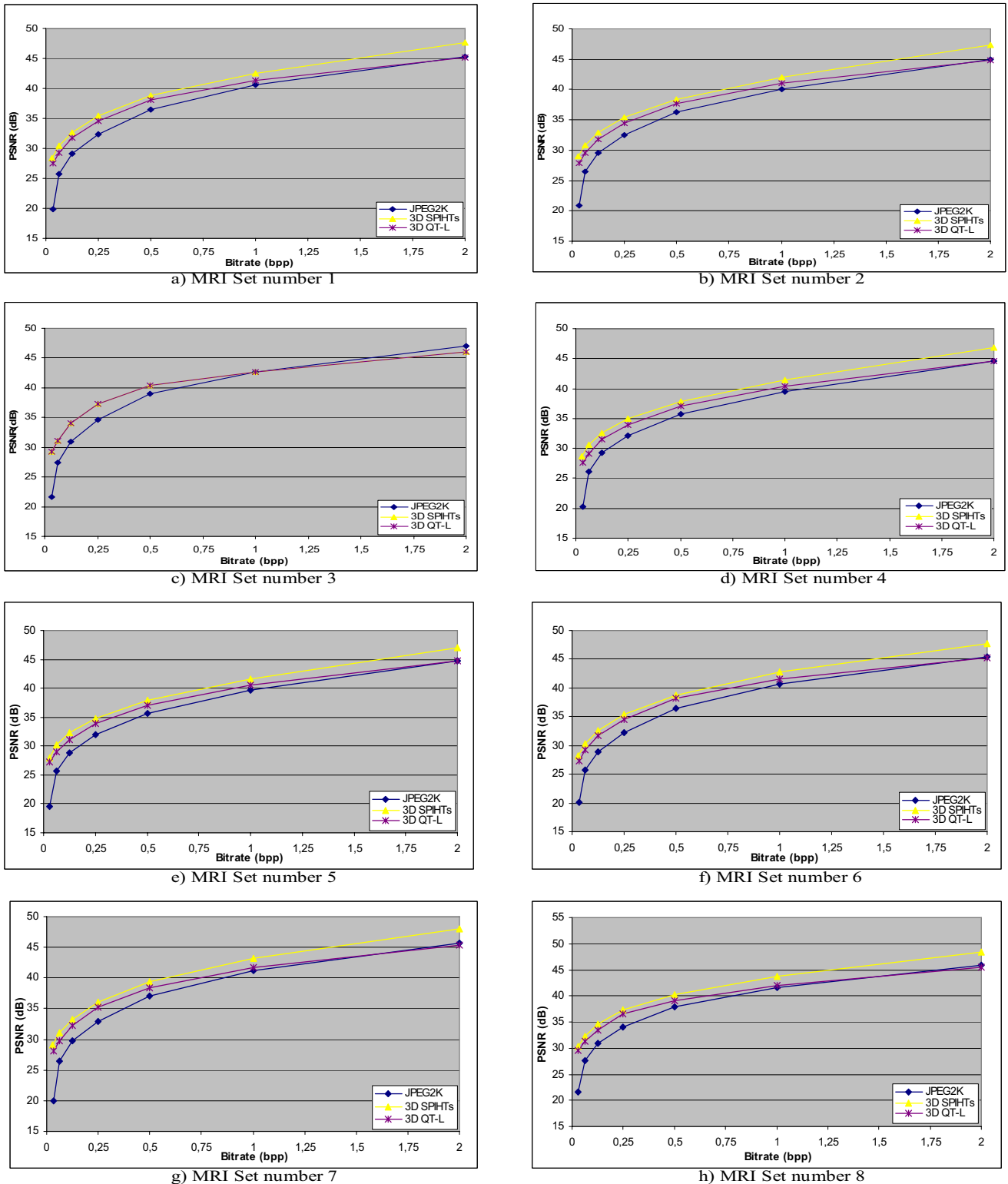


Fig. 5. The eight MRI datasets compressed with 3D SPIHTs, 3D QT-L and JPEG2K coders

At 2bpp bitrate, for all the datasets except for the dataset number 3, JPEG2K and 3D QT-L have nearly the same PSNR value. We must deduce from (Fig. 5) that the three coders have relatively the same behaviour, for the eight datasets.

Table 1 illustrates the compression results using the three coders. PSNR average value and the PSNR variance value are computed among the eight datasets, for each coder and each bitrate value.

In Table 1, we summarize the behaviour of the three coders for the average of the eight datasets. We can see that the PSNR variance value, for low bitrate values, is not very high. So, this confirms that the three coders perform relatively near results for the eight test datasets especially for low bitrate values.

Fig. 6. approves the obtained results by Table 1. It shows that the 3D SPIHT algorithm has the best PSNR average values, while the 3D QT-L is better than JPEG2K.

In addition, we will compare the performances of each coder, by measuring the encoding and decoding computing

time (Table 2). One can point out that JPEG2K coder requires less computing time than the other coders. While the 3D SPIHT uses less computing time than 3D QT-L. We must deduce that those encoding and decoding computing time are proportional to the requested memory for processing purpose. In fact JPEG2K performs the dataset compression for the 124 frames, frame by frame. So JPEG2K needs less time than 3D SPIHTs which performs the compression for a sixteen image group. While 3D QT-L achieves the compression of the 124 dataset images in one time so it spends more time than the two others.

TABLE I
 COMPRESSION RESULTS USING THE THREE CODERS. PSNR AVERAGE AND PSNR VARIANCE ARE AVERAGED OVER THE EIGHT DATASETS, FOR EACH CODER AND FOR EACH BITRATE VALUE

Bitrate(bpp)	JPEG2K		3D SPIHTs		3D QT-L	
	PSNR Average(dB)	PSNR Variance	PSNR Average(dB)	PSNR Variance	PSNR Average(dB)	PSNR Variance
0,03125	20,50	0,60	28,87	0,66	28,00	0,67
0,0625	26,40	0,62	30,94	0,80	29,74	0,72
0,125	29,65	0,70	33,19	0,96	32,17	0,96
0,25	32,83	0,95	35,85	1,17	35,01	1,37
0,5	36,80	1,27	39,05	1,31	38,23	1,01
1	40,75	1,18	42,70	1,15	41,39	0,49
2	45,41	0,59	47,79	0,66	45,16	0,20

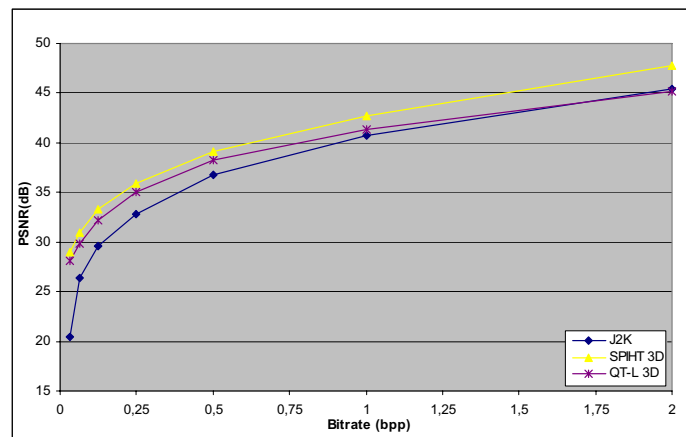


Fig. 6 Coding results using the 3D SPIHTs, 3D QT-L and JPEG2K coder. PSNR Average variation in decibels computed for the eight data sets as a function of bit-rate for the three coders.

Fig. 7. shows the visual results performed by the three coders 3D QT-L, 3D SPIHT and JPEG2K for low bitrates such as 0.125bpp, 0.0625bpp and 0.03125bpp. As a result, the 3D SPIHT and the 3D QT-L coders preserve more details than JPEG2K. Thus, it is very clear that for those three bitrate values, the reconstructed images by JPEG2K have bad

reconstruction quality than those reconstructed by the two other coders. In fact, for the other coders we loss some image details, especially for 0.0625 bpp and 0.03125 bpp. So for the purpose of tumour quantification, these bitrates are not appropriate.

TABLE II
 CODING TIME AND DECODING TIME VARIATIONS.
 COMPUTING TIMES ARE MEASURED FOR 3D SPIHTs, 3D QT-L AND JPEG2K CODERS FOR EACH BITRATE VALUE

Bitrate (bpp)	JPEG2K		3D SPIHTs		3D QT-L	
	Encoding time (s)	Decoding time (s)	Encoding time (s)	Decoding time (s)	Encoding time (s)	Decoding time (s)
0,03125	8,18	5,08	9,84	7,97	40,56	31,31
0,0625	7,99	5,13	9,84	8,37	47,28	36,66
0,125	7,57	5,52	9,69	8,14	50,79	39,83
0,25	7,68	6,19	9,84	8,20	57,78	42,52
0,5	7,03	7,08	10,82	8,96	66,85	55,89
1	7,07	8,33	11,24	9,29	66,31	55,91
2	7,18	10,09	16,30	12,93	71,09	60,40

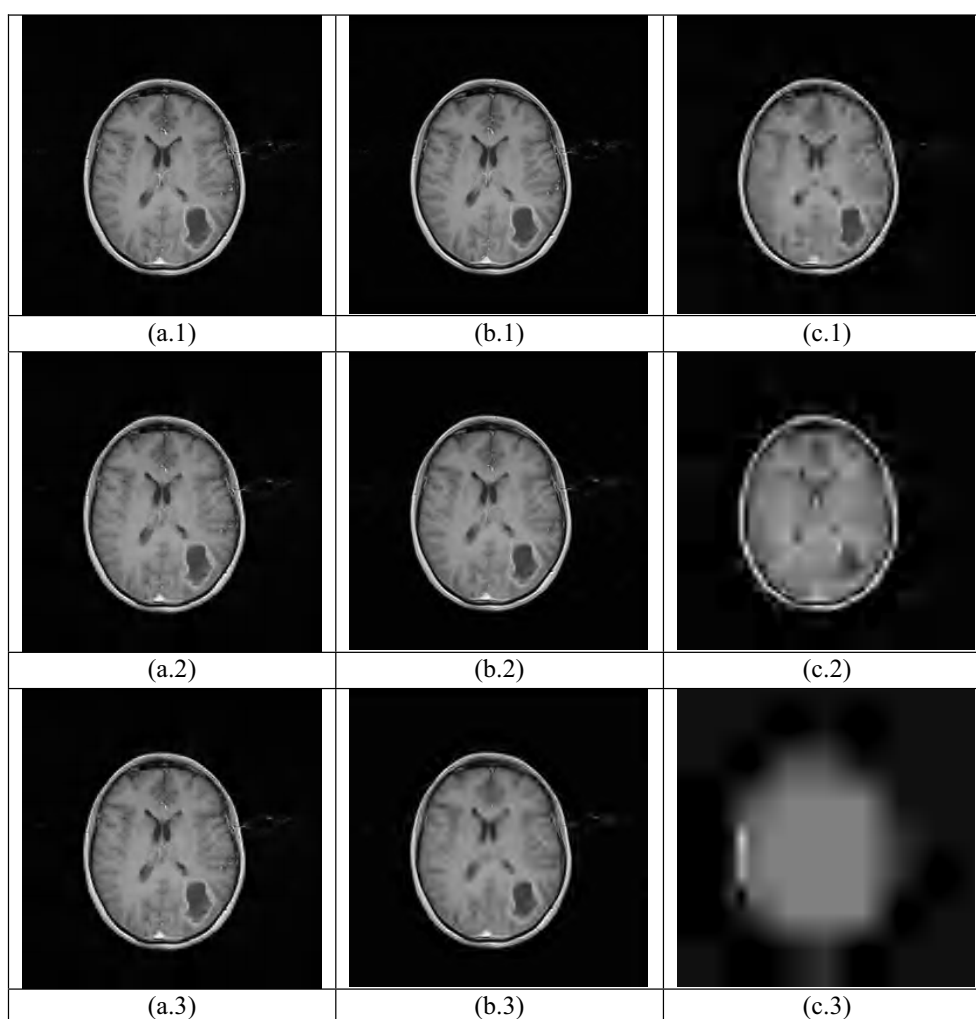


Fig. 7 Slice number 72 of MRI volume image data number 3 compressed at 1) 0.125bpp, 2) 0.0625bpp and 3) 0.03125bpp using (a) 3D QT-L, (b) 3D SPIHTs

A. Transmission results

Another test has been performed in order to evaluate the robustness of these algorithms face to coding errors. In this step, we tested the wireless transmission of the compressed images by two different coding algorithms such as JPEG2K

and 3D SPIHT coders. Hence, for this purpose, different bitrates and different Bit Error Rate (BER) have been used by considering both Gaussian and Rayleigh channels. The transmission is then performed according to an interleaving process. These transmission tests have been achieved only for acceptable quality of compressed images (i.e. 0.125 bpp).

1) AWGN channel

The transmission performance over AWGN wireless channel of 3D SPIHT and JPEG2K is reported in Table III. The robustness of coders over this channel is evaluated, in dB using the PSNR at the following bitrate values: 2, 1, 0.5, 0.25 and 0.125(bpp). Different BER values have also been considered, (Table III). Concerning JPEG2K, the transmitted image can't be reconstructed for a BER value higher than 10⁻⁴, whereas for 3D SPIHT, the transmitted and compressed

image can be reconstructed up to a BER value superior to 10⁻⁴. Therefore, one has to point out that using this coder, the quality of the reconstructed image is reduced starting from a BER value equal to 10⁻⁵. Moreover, some of the compressed images by JPEG2K and then transmitted can't be reconstructed. In table III, we summarize the results of the transmission of the dataset for different bitrates and different BER values. For the whole bitrate values, JPEG2K coder is higher than 3D SPIHT algorithm.

TABLE III
 PERFORMANCE COMPARISONS IN DB USING TWO CODING ALGORITHM 3D SPIHTS AND JPEG2K FOR TRANSMISSION OVER GAUSSIAN AND RAYLEIGH CHANNEL. PSNR VALUES MEASURED FOR EACH BER VALUE FOR DIFFERENT BITRATE VALUE

Bitrate (bpp)	GAUSSIAN CHANNEL				RAYLEIGH CHANNEL			
	3D SPIHTs		JPEG2K		3D SPIHT		JPEG2K	
	PSNR (dB)	TEB	PSNR (dB)	TEB	PSNR (dB)	TEB	PSNR (dB)	TEB
2	48,29	2,68E-07	40,86	3,88E-06	31,69	1,27E-05	45,38	1,40E-05
2	46,58	1,04E-06	38,87	1E-05	27,44	1,58E-05	39,89	1,71E-05
2	32,98	4,82E-06	37,61	2,95E-05			35,24	2,77E-05
2	26,48	1,27E-05	31,87	8,09E-05			28,54	5,57E-05
1	44,87	2,38E-07	38,01	3,01E-06	31,79	1,32E-05	42,20	1,26E-05
1	44,87	7,15E-07	36,58	6,71E-06	27,51	1,64E-05	39,76	1,58E-05
1	33,16	4,29E-06	35,43	2,98E-05			38,20	2,80E-05
1	26,53	1,18E-05	29,32	7,69E-05			31,19	6,42E-05
0,5	41,38	4,76E-07	34,93	3,72E-06	32,10	1,45E-05	38,85	1,22E-05
0,5	41,38	7,15E-07	34,26	7,12E-06	27,76	1,87E-05	37,80	1,93E-05
0,5	33,76	4,05E-06	34,26	2,57E-05			36,15	3,30E-05
0,5	26,69	1,18E-05	29,49	6,83E-05			29,66	7,33E-05
0,25	38,09	4,76E-07	34,28	7,71E-06	32,85	1,51E-05	34,64	1,20E-05
0,25	38,09	9,53E-07	34,28	7,71E-06	28,32	2,02E-05	33,39	2,71E-05
0,25	33,80	4,23E-06	34,28	1,13E-05			30,34	7,55E-05
0,25	27,11	1,21E-05	32,06	6,03E-05			23,85	2,38E-04
0,125	32,74	3,21E-06	29,79	1,54E-05	34,26	1,40E-05	31,02	2,62E-05
0,125	27,87	9,17E-06	29,79	1,54E-05	29,21	1,72E-05	30,61	4,44E-05
0,125	21,65	2,93E-05	29,79	1,54E-05			28,89	1,28E-04
0,125	18,78	8,04E-05	27,35	7,54E-05			25,42	3,55E-04

Some of the reconstructed after being transmitted dataset images are badly reconstructed (i.e. Presence of many artefacts) and for others, the image becomes unusable. On the other hand, for other frames, the image is properly reconstructed. This is in fact observed for the BER values superior to 10⁻⁵, especially for the JPEG2K coder when the dataset images are transmitted over a Gaussian wireless channel (Fig. 8.).

The transmission of 3D SPIHT compressed images over Gaussian channel, leads continually to low quality reconstructed images, when the BER value is more than 2 10⁻⁵ (Fig. 9).

2) Rayleigh channel

In this subsection, the transmission test, is performed over Rayleigh channel. Therefore, one can note that for this channel model, JPEG2K has higher PSNR values in comparison to those measured using 3D SPIHT (Table III). Although, some of the dataset images are reconstructed with a modified image size, some others cannot be reconstructed.

For the 3D SPIHT, the reconstructed image is destroyed beyond a BER value of 1,63 10⁻⁵. The compressed image by 3D SPIHT through Rayleigh Channel, cannot be transmitted using a BER value less than 6 10⁻⁵.

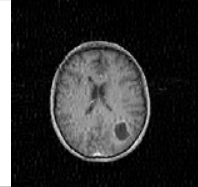
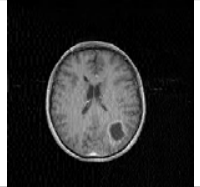
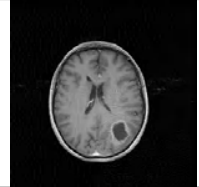
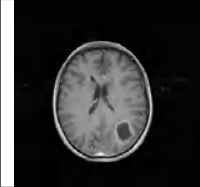

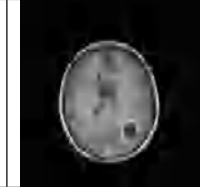
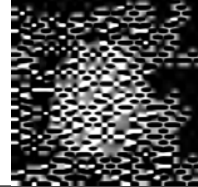
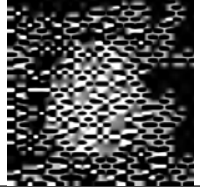
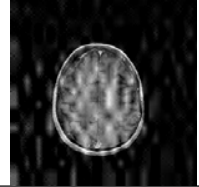
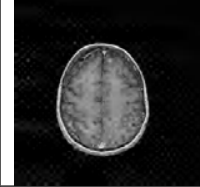
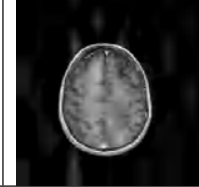
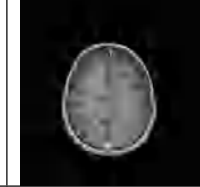
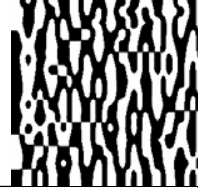
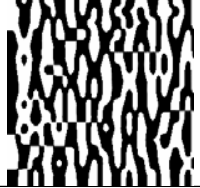
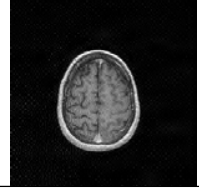
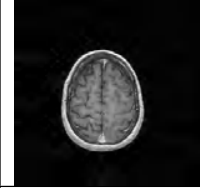
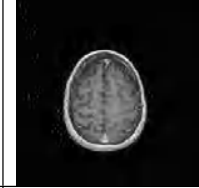

					
Slice_75, Bitrate(2bpp), BER($8.26 \cdot 10^{-5}$), PSNR(29.54db)	Slice_75, Bitrate(1bpp), BER($7.45 \cdot 10^{-5}$), PSNR (30.79 db)	Slice_75, Bitrate(0.5bpp), BER($7.03 \cdot 10^{-5}$), PSNR (34.99 db)	Slice_75, Bitrate(0.25pp), BER($4.61 \cdot 10^{-5}$), PSNR (33.45db)	Slice_75, Bitrate(0.125pp), BER($7.61 \cdot 10^{-5}$), PSNR(24.70db)	Slice_75, Bitrate(0.0625bpp), BER($6.18 \cdot 10^{-5}$), PSNR(25.01db)
					
Slice_90, Bitrate(2bpp), BER($8.12 \cdot 10^{-5}$), PSNR(9.05db)	Slice_90, Bitrate(1bpp), BER($8.17 \cdot 10^{-5}$), PSNR(9.04 db)	Slice_90, Bitrate(0.5bpp), BER($7.09 \cdot 10^{-5}$), PSNR(21.94 db)	Slice_90, Bitrate(0.25bpp), BER($6.88 \cdot 10^{-5}$), PSNR(29.72 db)	Slice_90, Bitrate(0.125bpp), BER($7.75 \cdot 10^{-5}$), PSNR(25.83 db)	Slice_90, Bitrate(0.0625bpp), BER($6.37 \cdot 10^{-5}$), PSNR(25.55 db)
					
Slice_99, Bitrate (2bpp), BER($8.19 \cdot 10^{-5}$), PSNR(3.65db)	Slice_99, Bitrate (1bpp), BER($7.59 \cdot 10^{-5}$), PSNR(3.65db)	Slice_99, Bitrate (0.5bpp), BER($7.02 \cdot 10^{-5}$), PSNR (29.89db)	Slice_99, Bitrate (0.25bpp), BER($6.90 \cdot 10^{-5}$), PSNR(32.75db)	Slice_99, Bitrate (0.125bpp), BER($7.72 \cdot 10^{-5}$), PSNR(29.39db)	Slice_99, Bitrate (0.0625bpp), BER($9.11 \cdot 10^{-5}$), PSNR(24.91db)

Fig. 8 Visual comparisons of different dataset slices using JPEG2K transmitted over Gaussian wireless channel. for different bitrate values and BER values.

We must conclude that for JPEG2K compressed images, some of the reconstructed images present artefacts whereas others can't be reconstructed. On the other hand, when using

3D SPIHT, the compressed and transmitted image reconstruction is very sensitive to the BER variation (Fig.10).


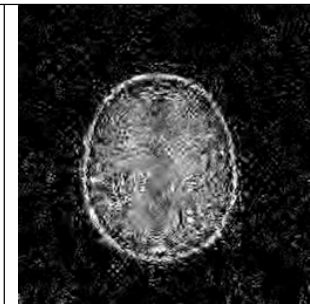
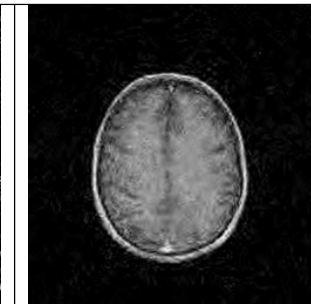

			
BER= $9.04 \cdot 10^{-5}$ PSNR=17.54dB	BER= $3.58 \cdot 10^{-5}$ PSNR=17.64 dB	BER= $1.30 \cdot 10^{-5}$ PSNR=26.47 dB	BER= $4.76 \cdot 10^{-6}$ PSNR=27.57 dB

Fig. 9 Visual comparisons of slice number 82 of the MRI dataset number 3 using 3D SPIHTs transmitted over Gaussian wireless channel for bitrate equal to 2 bpp.

I. CONCLUSION

In this work, wavelet based coding methods have been considered. The performances have been evaluated in case of image transmission over various wireless channels. Therefore,

three wavelet based coders has been tested, namely 3D QT-L, 3D SPIHT and JPEG2K. Moreover, eight MRI dataset images have been considered for this study. As it has been seen previously, 3D SPIHT provides best performances for the

whole tested bitrate values, whereas we have shown that 3D QT-L outperforms clearly JPEG2K.

In case of wireless transmission, coder robustness has been evaluated for 3D SPIHT and JPEG2K coder. It has been shown that JPEG2K is more robust regarding coding errors, in spite of the impossibility to reconstruct some images. While, it becomes apparent that 3D SPIHT, is very sensitive to BER variation and images. Therefore, 3D SPIHT is not very robust to wireless transmission. We may conclude then, the necessity of including corrector codes in order to protect the transmitted information. This would guaranty a diagnostic accuracy when the medical image dataset must be transmitted.

REFERENCES

[1] D. Tzovaras, N. Grammalidis, M.G. Strintzis and S. Malassiotis, « Coding for the storage and communication of visualisations of 3D medical data », *Signal Processing : Image Communication*, Vol. 13, pp. 65-78, 1998.

[2] S.-G. Miaou, S.-T. Chen, "Automatic Quality Control for Wavelet-Based Compression of Volumetric Medical Images Using Distortion-Constrained Adaptive Vector Quantization", *IEEE Trans. on Medical Images Using Distortion-Constrained Adaptive Vector Quantization*, Vol. 23, No 11, Nov. 2004.

[3] L.W.C. Chan, M.Z. Zhou, S.K. Hau, M.Y.Y. Law, F.H. Tang and J. Documet, "International Internet-2 performance and automatic tuning protocol for medical imaging applications", *Computerized Medical Imaging and Graphics*, Vol. 29, pp. 103-114, 2005.

[4] X. Qi and J.M. Tyler, "A progressive transmission capable diagnostically lossless compression scheme for 3D medical image sets, *Information Sciences*, Vol. 175, pp. 217-243, 2005.

[5] B. Ramakrishnan and N. Sriraam, "Internet transmission of DICOM images with effective low bandwidth utilization", *Digital Signal Processing*, Vol. 16, pp. 825-831, 2006.

[6] J. M. Shapiro, "Embedded image coding using zerotrees of wavelet coefficients," *IEEE Trans. Signal Processing*, vol. 41, pp. 3445-3462, 1993.

[7] K.R. Namuduri and V.N. Ramaswamy, "Feature preserving image compression", *Pattern Recognition Letters*, Vol. 24, pp. 2767-2776, 2003.

[8] A. Said and W. Pearlman, "A new fast and efficient image codec based on set partitioning in hierarchical trees," *IEEE Trans. Circuits Syst. Video Technol.*, vol. 6, pp. 243-250, June 1996.

[9] M. Penedo, W.A. Pearlman, P.G. Tahoces, M. Souto and J.J. Vidal, "Region-Based Wavelet Coding Methods for Digital Mammography", *IEEE Trans. on Medical Imaging*, Vol. 22, No. 10, pp. 1288-1296, Oct. 2003.

[10] W.A. Pearlman, A. Islam, N. Nagaraj and A.Said, "Efficient, low-complexity image coding with a set-partitioning embedded block coder", *IEEE Trans. Circuits and Syst. Video Technol.*, Vol 14, No 11, pp. 1219 - 1235, Nov. 2004.

[11] D. Taubman, "High performance scalable image compression with EBCOT", *IEEE Trans. on Image Processing*, vol. 9, No. 7, pp. 1158-70, Jun 2000.

[12] C. Christopoulos, A. Skodras and T. Ebrahimi, "The JPEG2000 Still image coding system: An overview", *IEEE Trans. on Consumer Electronics*, Vol. 46, No. 4, pp. 1103-1127, Nov. 2000.

[13] N. Thomos, N. V. Boulgouris and M. G. Strintzis, "Optimized Transmission of JPEG2000 streams over wireless channels", *IEEE Trans. on Image Processing*, vol. 15, No1, pp. 54-67, Jan 2006.

[14] K. Krishnan, M.W. Marcellin, A. Bilgin and M.S. Nadar, "Efficient Transmission of Compressed Data for Remote Volume Visualization", *IEEE Trans. on Medical Imaging*, Vol. 25, No. 9, pp. 1189-1199, Sep. 2006

[15] Y. Zhang, B.T. Pham and M. P. Eckstein, "Automated Optimization of JPEG2000 Encoder Options Based on Model Observer Performance for Detecting Variable Signals in X-Ray Coronary Angiograms", *IEEE Trans. on Medical Imaging*, Vol. 23, No 4, pp. 459-474, April 2004.

[16] P. Schelkens, A. Munteanu, J. Barbarien, G. Mihneai, X. Giro-Nieto and J. Cornelis, "Wavelet coding of volumetric medical datasets", *IEEE Trans. on Medical Imaging*, vol. 22, No3, pp. 441-458, March 2003.

[17] A. Munteanu, "Wavelet Image Coding and Multiscale Edge Detection Algorithms and Applications", Ph.D dissertation, Vrije Univ. Brussel, Brussels, Belgium, 2003.

[18] G. Menegaz and J.-P. Thiran, "Lossy to Lossless Object-Based Coding of 3-D MRI Data", *IEEE Trans. on Image Processing*, vol.11, Septembre 2002.

[19] G. Menegaz and J.-P. Thiran, "Three-Dimensional Encoding/Two-Dimensional Decoding of Medical Data", *IEEE trans. on Medical Imaging*, vol. 22, no 3, March 2003.

[20] Y.S. Kim and W.A. Pearlman, "Stripe-based SPIHT compression of volumetric medical images for low memory usage and uniform reconstruction quality", in *Proc ICASSP*, vol 4, Jun. 2000, pp. 2031-2034.

[21] Z. Xiong, X. Wu, S. Cheng and J. Hua, "Lossy-to-Lossless Compression of Medical volumetric Data Using Three-dimensional Integer Wavelet Transforms", *IEEE Trans. on Medical Imaging*, vol.22, No3, pp. 459-470, March 2003.

[22] M. G. Strintzis, "A review of compression methods for medical images in PACS", *International Journal of Medical Informatics*, Vol. 52, No1, pp. 159-165, Oct. 1998.

[23] P. J. Klutke, P. Mattioli, F. Baruffaldi, A. Toni and K.-H. Englemeier, "The Telemedicine benchmark—a general tool to measure and compare the performance of video conferencing equipment in the telemedicine area", *Computer Methods and Programs in Biomedicine*, Vol. 60, no 2, pp. 133-141, 1999.

[24] C.N. Doukas, I. Maglogiannis and G. Kormentzas, "Medical Image Compression using wavelet Transform on Mobile Devices with ROI coding support", 27th Annual International Conference of the Engineering in Medicine and Biology Society, IEEE-EMBS 2005, pp. 3779-3784.

[25] J.H. Kim and J.K. Lee, "Capture Effects of Wireless CSMA/CA Protocols in Rayleigh and Shadow Fading Channels", *IEEE Trans. on Vehicular Technology*, Vol. 48, No. 4, pp. 1277-1286, July 1999.

[26] D. Wang, Y. Zhou, P. Su and J. Wang, "Robust Progressive Image Transmission Over Rayleigh Fading Channels", *International Conference on Communication Technology Proceedings*, 2003. ICCT 2003, Vol. 2, No. 9-11, pp. 846 - 849, April 2003.

[27] L.C. Ramac, "Performance of the Wavelet Domain Diversity Method for Image Transmission over Rayleigh Fading Channels", 2000 IEEE International Conference on Personal Wireless Communications, pp. 543 547, 2000.

[28] A. Naït-Ali and C. Cavaro-Ménard, «Compression des images et des signaux médicaux », Hermes Science Publications, Fev 2007.

[29] N. Thomos, N.V. Boulgouris and M.G.Strintzis, "Wireless image transmission using turbo codes and optimal unequal error protection", Vol. 14, No. 11, 2005. International Conference on Image Processing ICIP 2003. Proceedings, Vol. 1, No. 14-17, pp. 73-76, 2003.

[30] Medical Database for the Evaluation of Image and Signal processing (MeDEISA), http://www.istia.univ-angers.fr/LISA_MeDEISA/IEEE_FRANCE_EMB/

[31] E. Kofidis, N. Kolokotronis, A. Vassilarakou, S. Theodoridis and D. Cavouras, "Wavelet-based medical image compression", *Future Generation Computer Systems*, vol 15, No2, pp. 223-243, March 1999.

[32] M. Barlaud, "Compression et codage des images et des videos", Hermes 2002.

[33] Y. Gaudreau, "Contributions en compression d'images médicales 3D et d'images naturelles 2D", Ph.D dissertation, Henri Poincaré Univ., Nancy, France, 2006.

[34] American College of Radiology (ACR), "ACR technical standard for teleradiology", *ACR Practice Guideline*, pp. 801-810, Oct. 2005, www.acr.org.

[35] Erickson B.J, "Irreversible compression of medical images", *Journal of Digital Imaging*, vol. 15, no 1, pp. 5-14, March 2002.

[36] A.S. Tolba, "Wavelet Packet Compression of Medical Images", *Digital Signal Processing*, Vol. 12, pp. 441-470, 2002.